

Supporting Information (SI)

**Revealing the Conformational
Preferences of Proteinogenic Glutamic Acid
Derivatives in Solution by ^1H NMR
Spectroscopy and Theoretical Calculations**

Wesley G. D. P. Silva^{a,b}, Cláudio F. Tormena^a and Roberto Rittner^{a*}

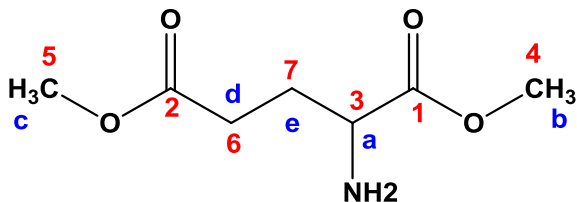
^aChemistry Institute, University of Campinas, Campinas, São Paulo 13083–970,
Brazil

^bDepartment of Chemistry, University of Manitoba, Winnipeg, Manitoba R3T
2N2, Canada

*Corresponding author: rittner@iqm.unicamp.br

Procedures for the Synthesis of the Compounds

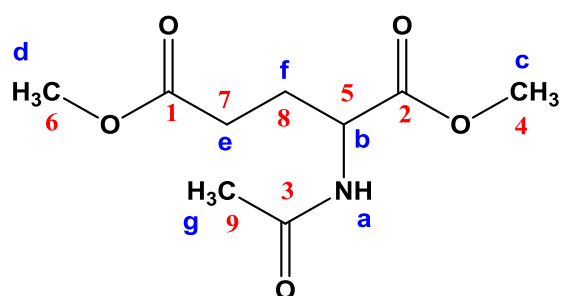
L-Glutamic Acid Dimethyl Ester (*GluOMe*)



Activated zinc dust (100 mg) was added to a suspension of the *L*-glutamic acid dimethyl ester hydrochloride (175.1 mg,

1.0 mmol) in 10 mL of dichloromethane. The reaction mixture was stirred for 3 h at room temperature. Then, the mixture was filtered, and the solvent was evaporated *in vacuo*. The amino acid ester free amine was obtained as a colorless liquid (191.5 mg, 0.8 mmol, 79.7 % yield), which was used without any further purification. **¹H NMR** (600.17 MHz, CD₃CN, 25 °C, TMS): δ (ppm) = Ha: 3.79 (t, ³J= 6.4Hz); Hb: 3.73 (s, 3H); Hc: 3.63 (s, 3H); Hd: 2.49 (ddd, ³J= 6.9 and 8.3 Hz, ²J= 16.9 Hz, 1H); Hd': 2.42 (ddd, ³J= 6.8 and 8.0 Hz, ²J= 16.9 Hz, 1H); He: 2.08 (m, 2H). **¹³C NMR** (150.91 MHz, CD₃CN, 25 °C, TMS): δ (ppm) = C1: 173.45; C2:172.64; C3: 53.12; C4: 52.19; C5: 51.01; C6: 29.07; C7: 27.74. **HRMS** (TOF-ES+): *m/z* [M+H]⁺ calculated for C₇H₁₄NO₄: 176.0878; found: 176.0919.

N-acetyl-L-glutamic acid dimethyl ester (*AcGluOMe*)



Thionyl chloride (0.7 mL, 9.6 mmol) was carefully added to a stirred solution of *N*-acetyl-L-glutamic acid (1.0 g, 5.2 mmol) in 10 mL of anhydrous MeOH. The reaction

mixture was stirred for 3 h at 0 °C and then at room temperature for further 24 h. The solvent was removed under reduced pressure, and 5 mL of water was added to the resulting residue followed by the washing with a saturated aqueous solution of KHCO_3 . The aqueous layer was extracted with dichloromethane (3 x 5 mL), and the combined organic layers were dried with anhydrous MgSO_4 , filtered and concentrated *in vacuo* to afford *N*-acetyl-L-glutamic acid dimethyl ester (453.5 mg, 2.1 mmol, 40.4 % yield) as a white solid. $^1\text{H NMR}$ (600.17 MHz, CD_3CN , 25 °C, TMS): δ (ppm) = Ha: 6.71 (s, 1H); Hb: 4.37 (ddd, $^3J = 5.3, 7.9$ and 8.7 Hz, 1H); Hc: 3.66 (s, 3H); Hd: 3.62 (s, 3H); He: 2.37 (m, 2H); Hf: 2.07 (m, 1H); Hf': 1.87 (m, 1H); Hg: 1.89 (m, 3H). $^{13}\text{C NMR}$ (150.91 MHz, $\text{DMSO-}d_6$, 25 °C, TMS): δ (ppm) = C1: 174.34; C2: 173.69; C3: 171.28; C4: 53.13; C5: 52.94; C6: 52.55; C7: 31.03; C8: 27.87; C9: 23.12. **HRMS** (TOF-ES+): m/z $[\text{M} + \text{H}]^+$ calculated for $\text{C}_9\text{H}_{16}\text{NO}_5$: 218.0984; found: 218.1003.

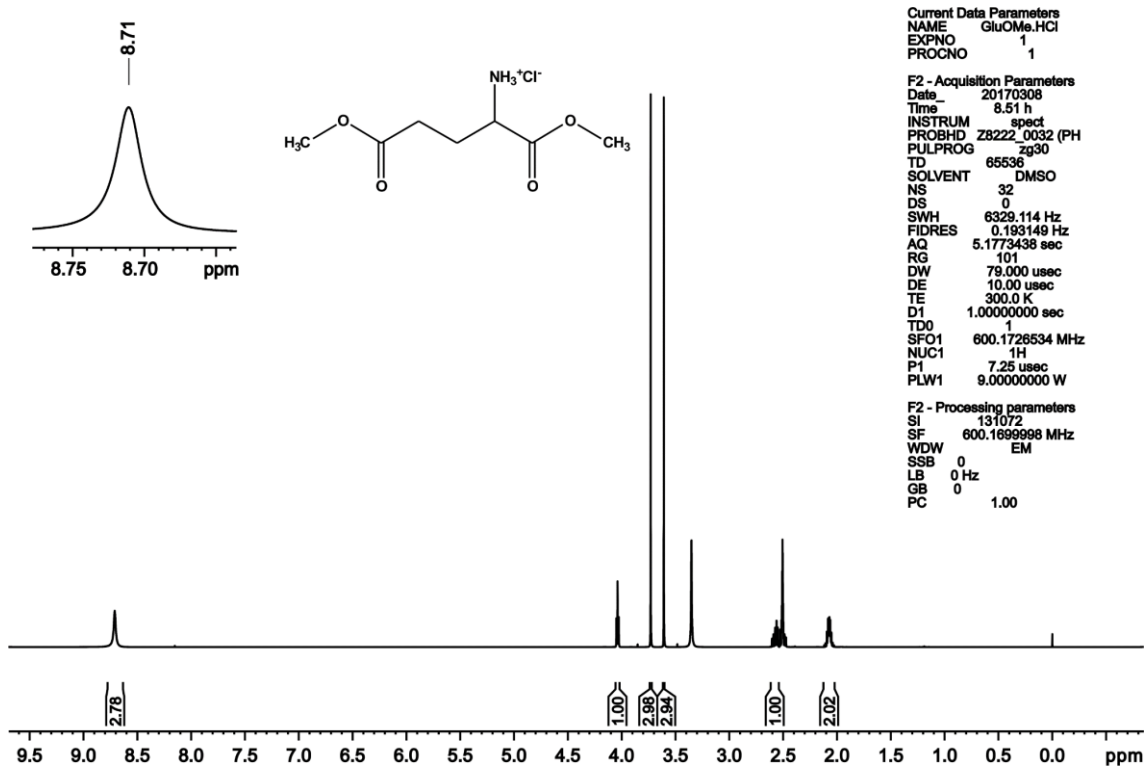


Figure S1 ¹H NMR spectra of GluOMe.HCl in DMSO-*d*₆.

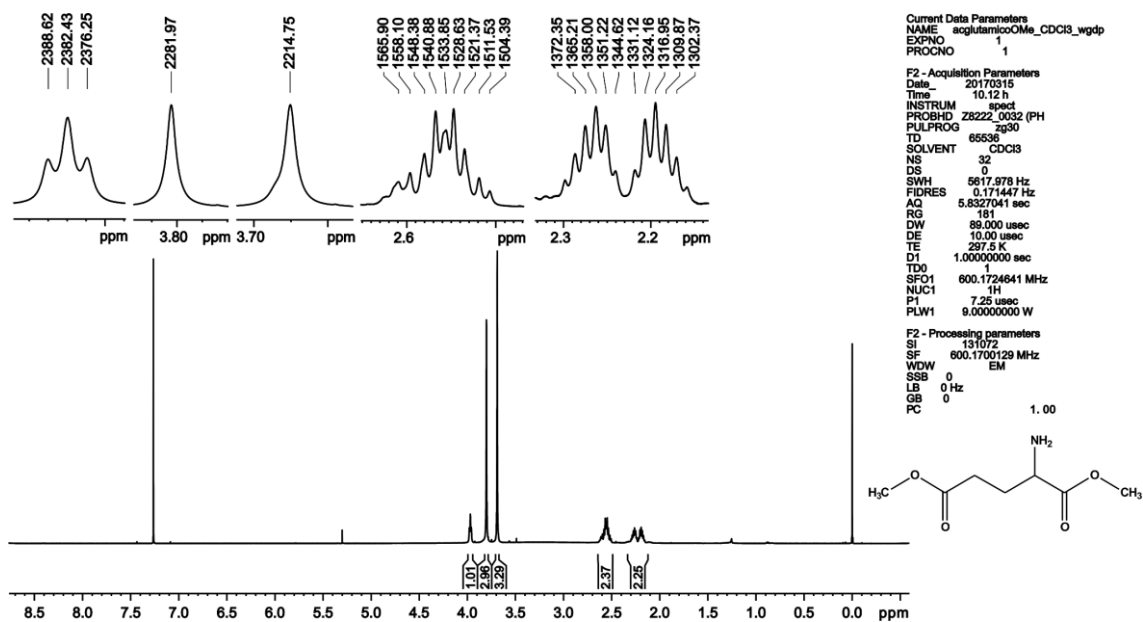


Figure S2 ¹H NMR spectra of GluOMe in CDCl₃.

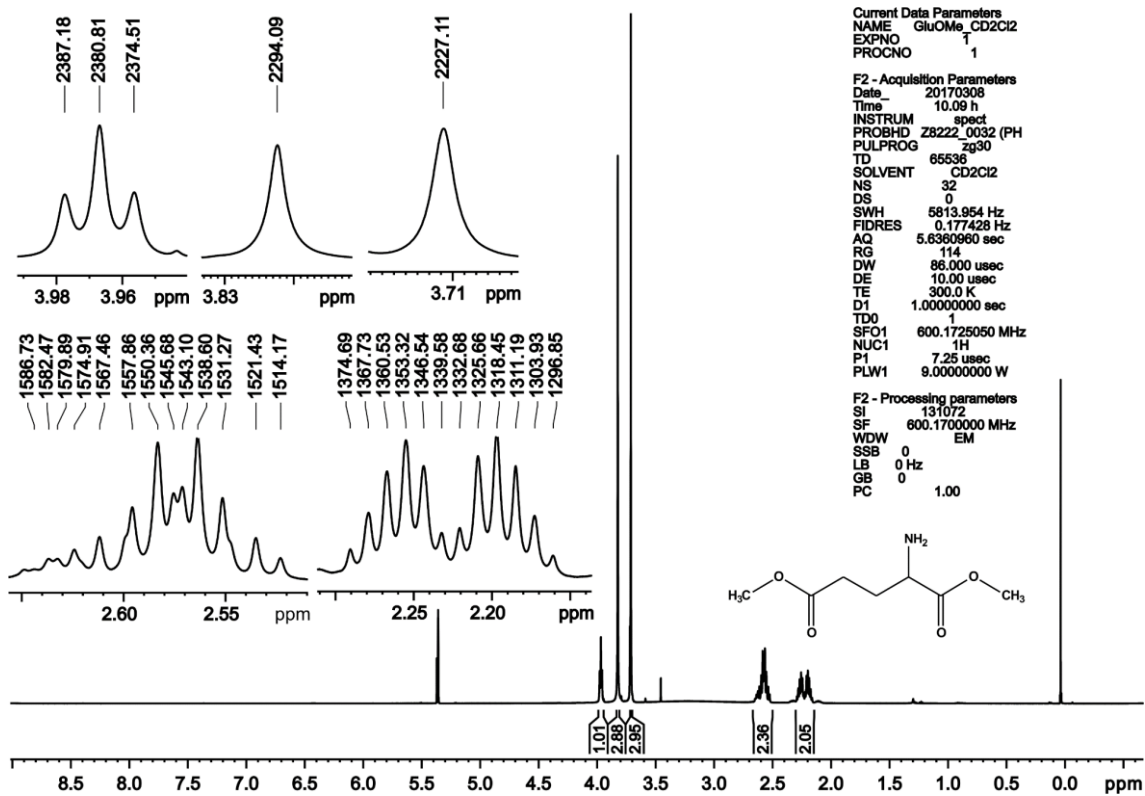


Figure S3 ¹H NMR spectra of GluOMe in CD₂Cl₂.

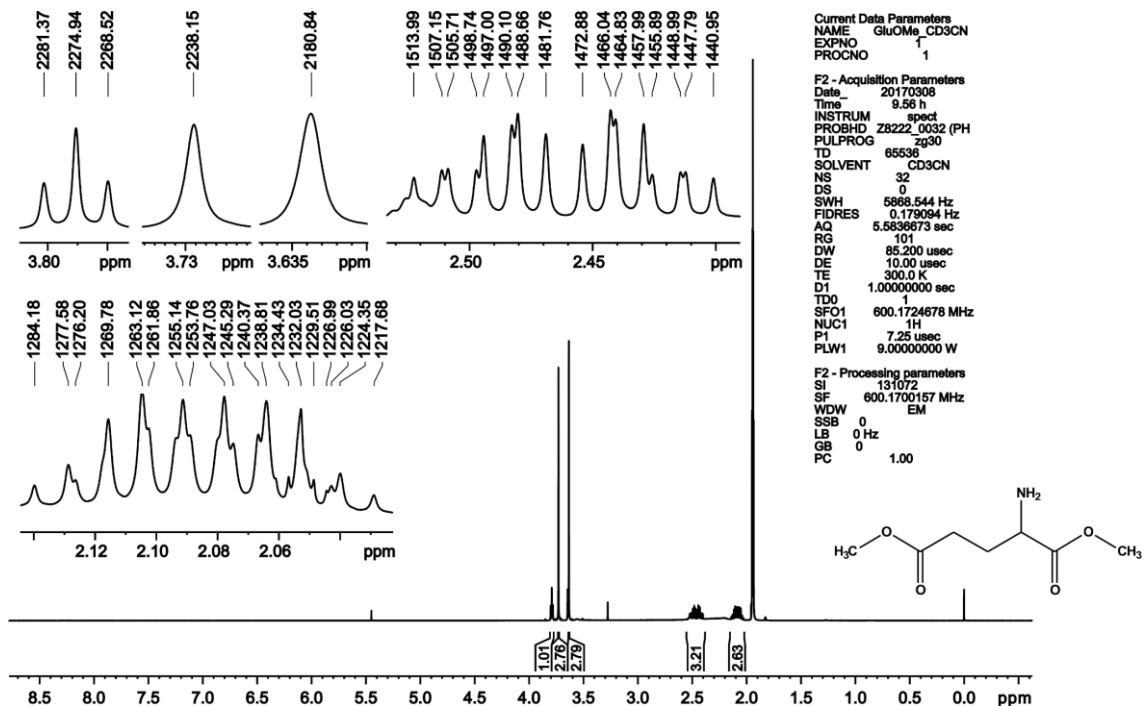


Figure S4 ¹H NMR spectra of GluOMe in CD₃CN.

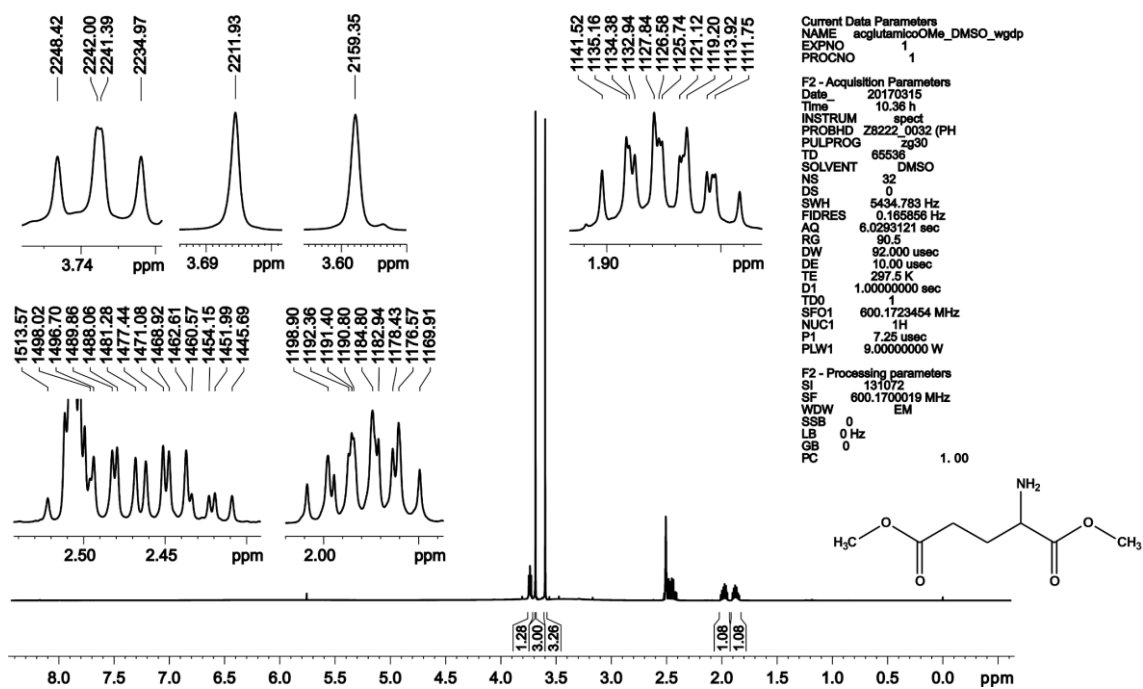


Figure S5 ^1H NMR spectra of GluOMe in $\text{DMSO}-d_6$.

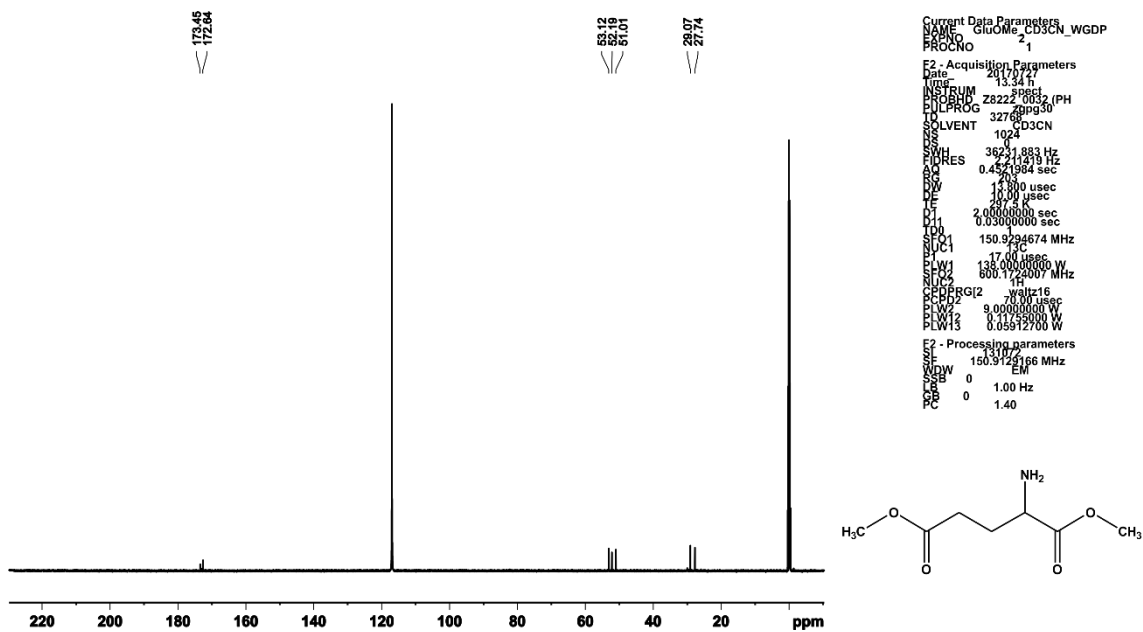


Figure S6 ^{13}C NMR spectra of GluOMe in CD_3CN .

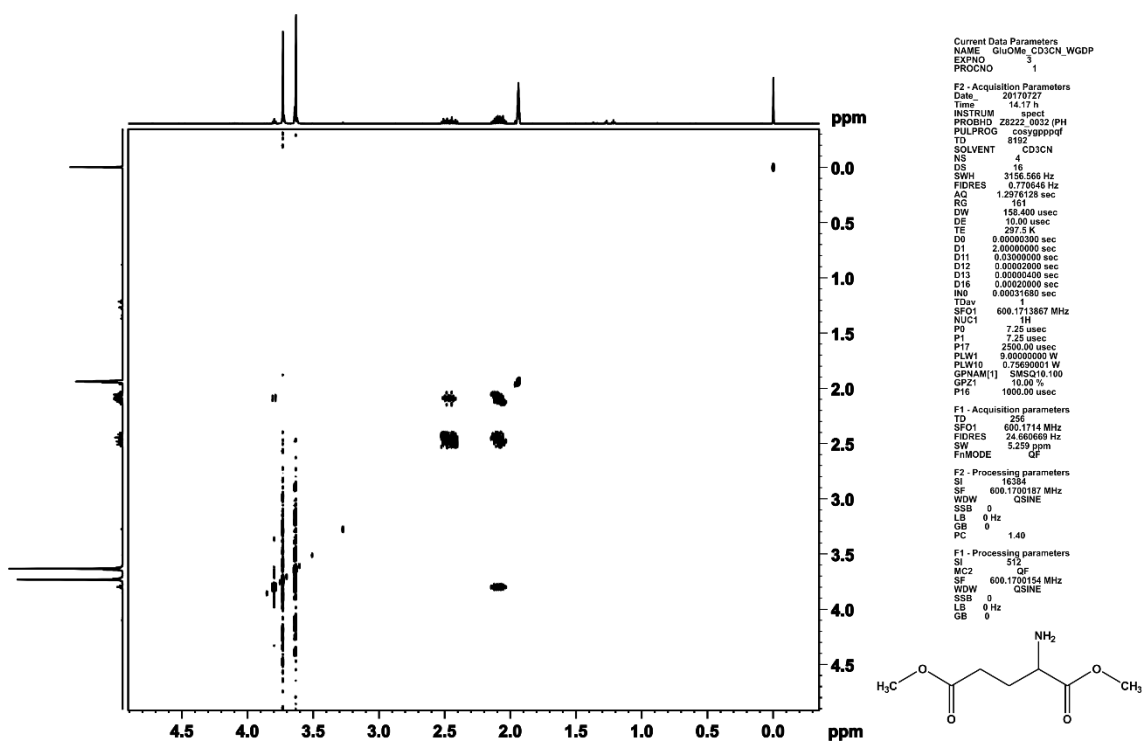


Figure S7 COSY contour plot of GluOMe in CD₃CN.

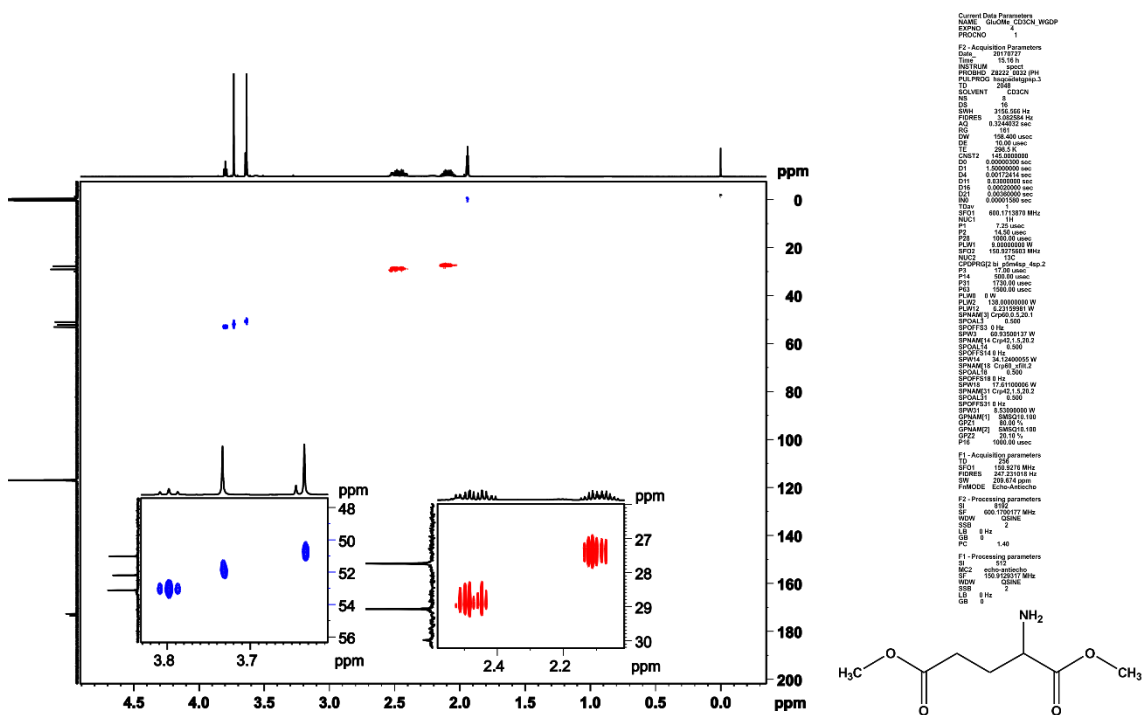


Figure S8 HSQC contour plot of GluOMe in CD₃CN (red cross peaks refer to CH₂ and blue cross peaks refer to CH or CH₃).

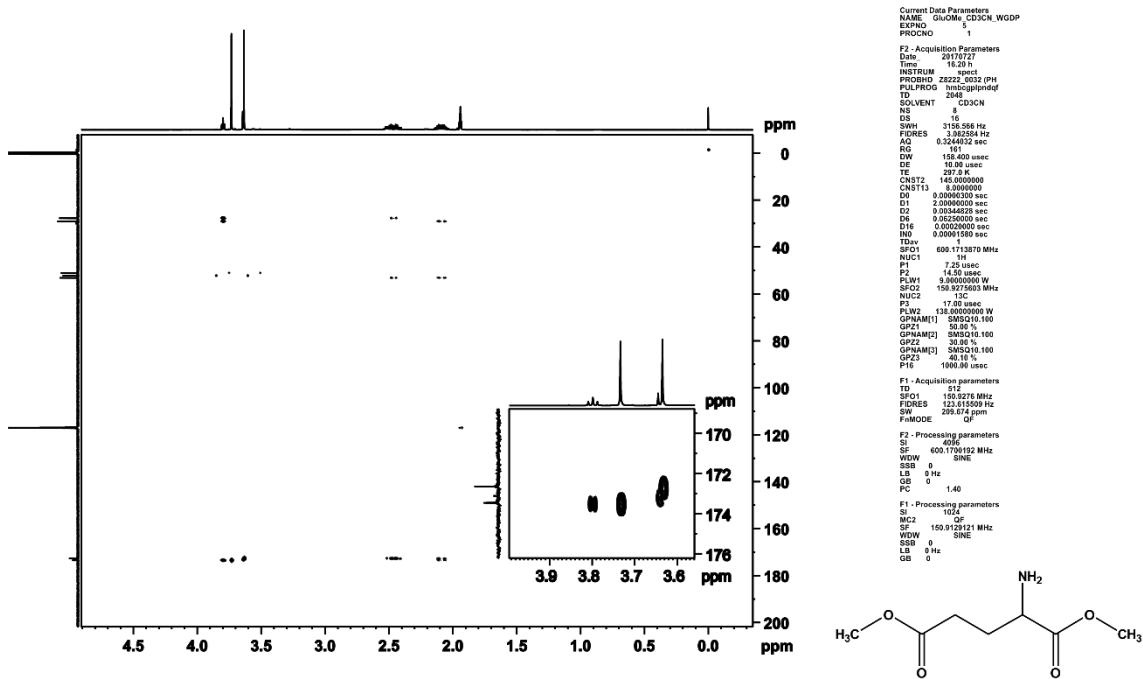


Figure S9 HMBC contour plot of GluOMe in CD₃CN.

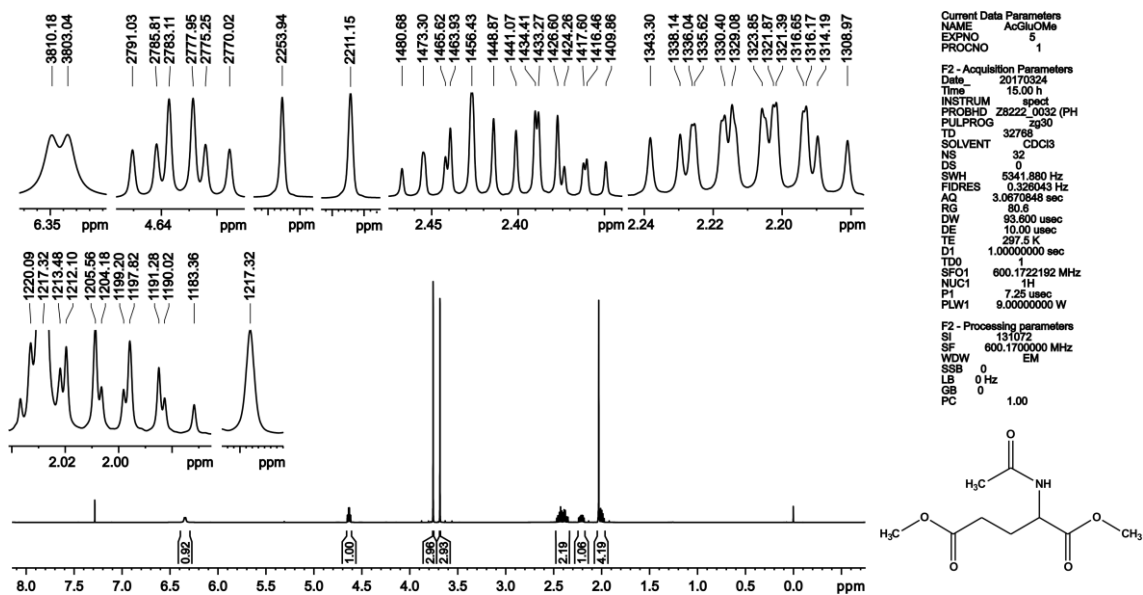


Figure S10 ¹H NMR spectra of AcGluOMe in CDCl₃.

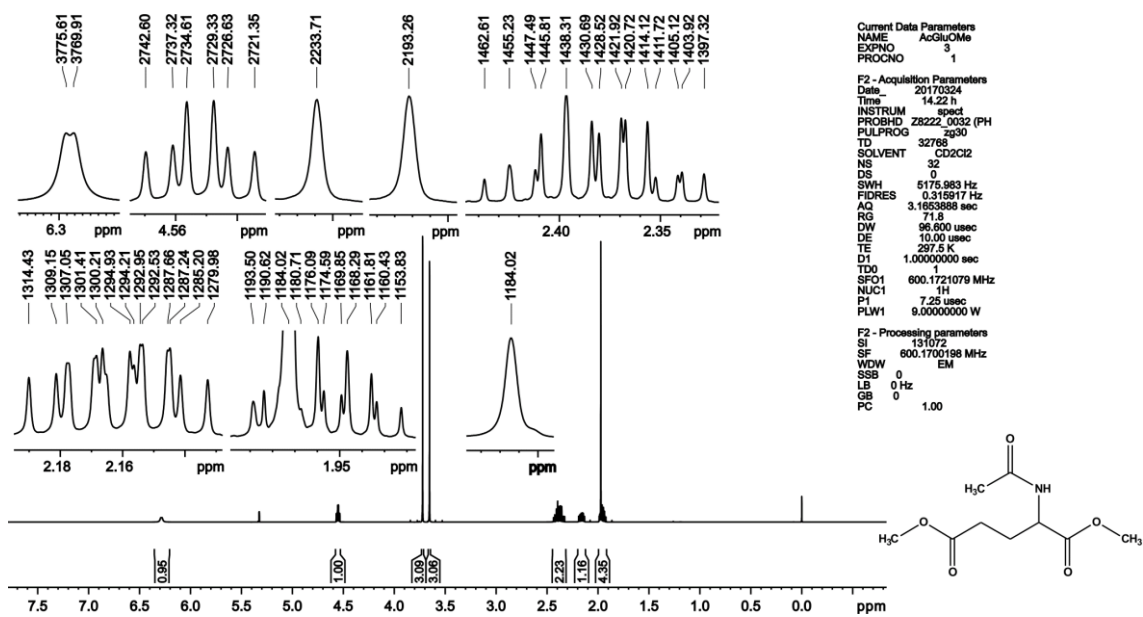


Figure S11 ¹H NMR spectra of AcGluOMe in CD₂Cl₂.

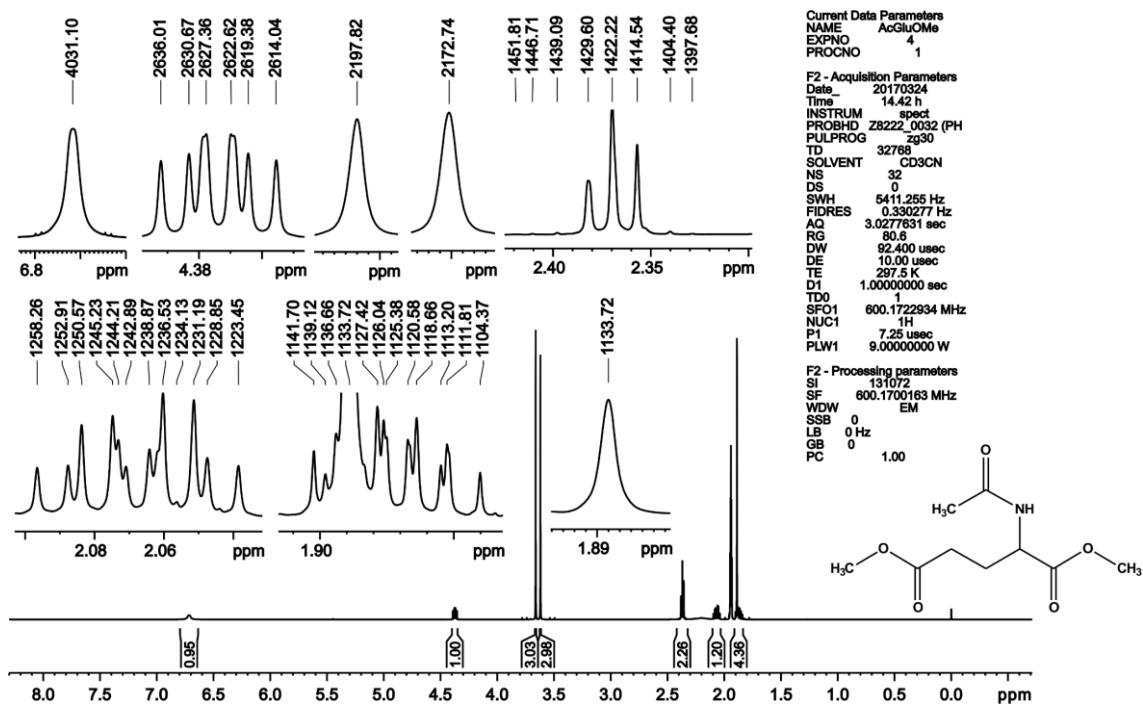


Figure S12 ¹H NMR spectra of AcGluOMe in CD₃CN.

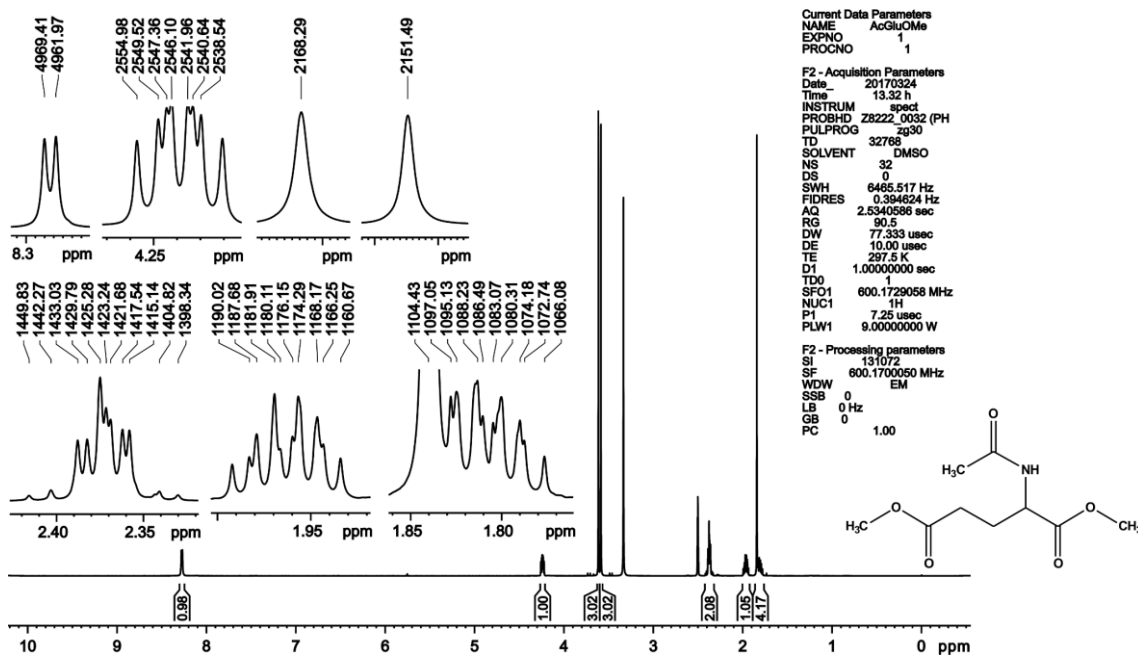


Figure S13 ^1H NMR spectra of AcGluOMe in $\text{DMSO-}d_6$.

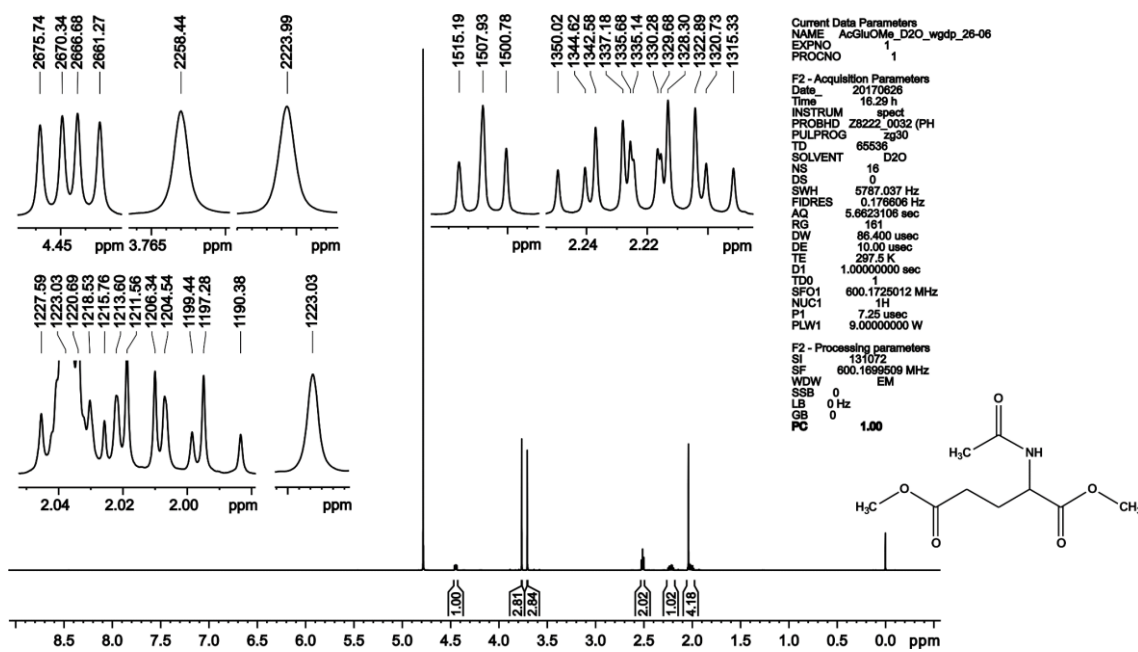


Figure S14 ^1H NMR spectra of AcGluOMe in D_2O .

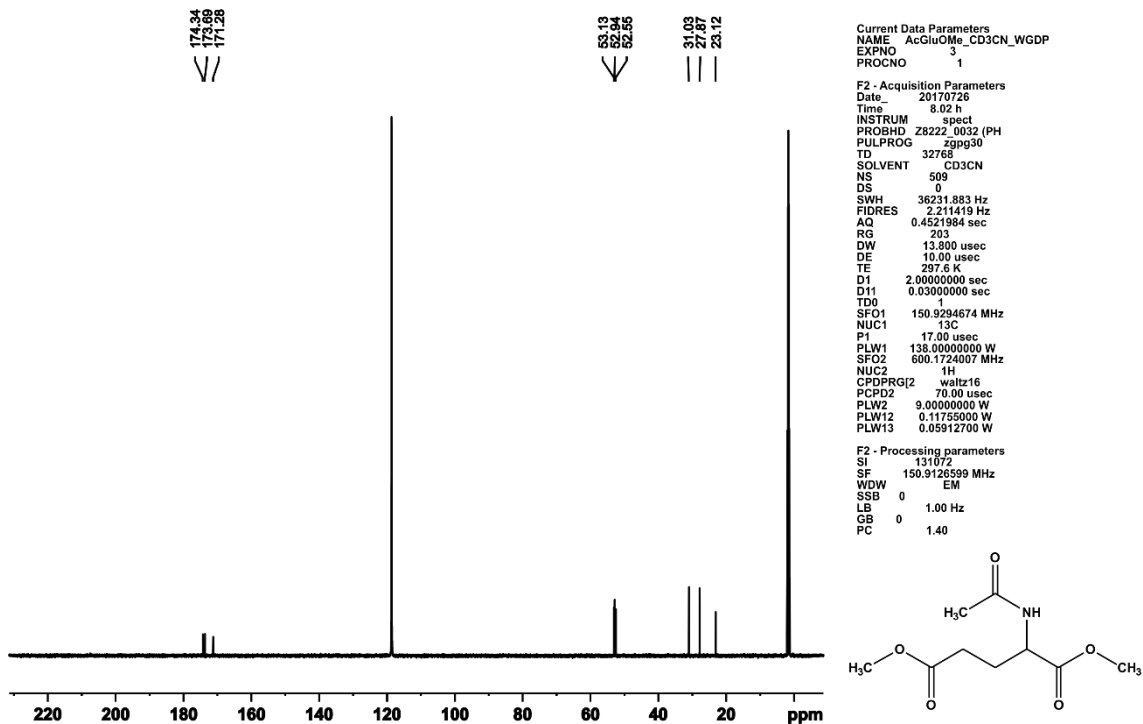


Figure S15 ^{13}C NMR spectra of AcGluOMe in CD_3CN .

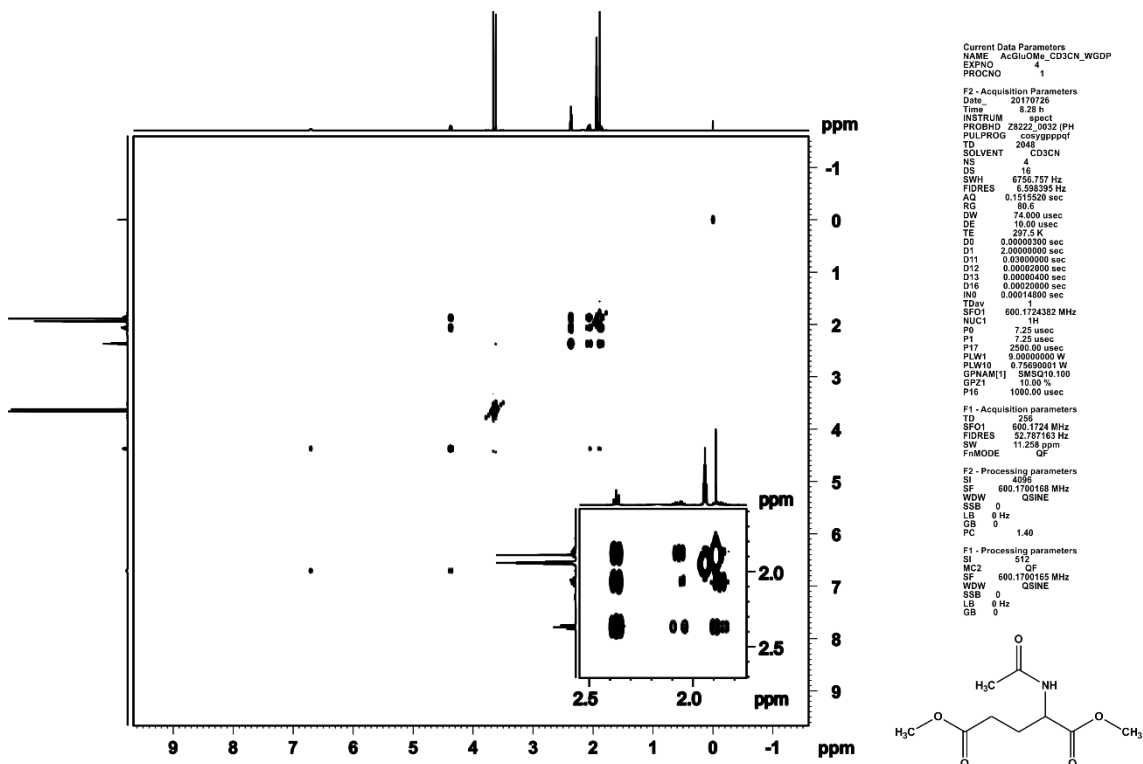


Figure S16 COSY contour plot of AcGluOMe in CD_3CN .

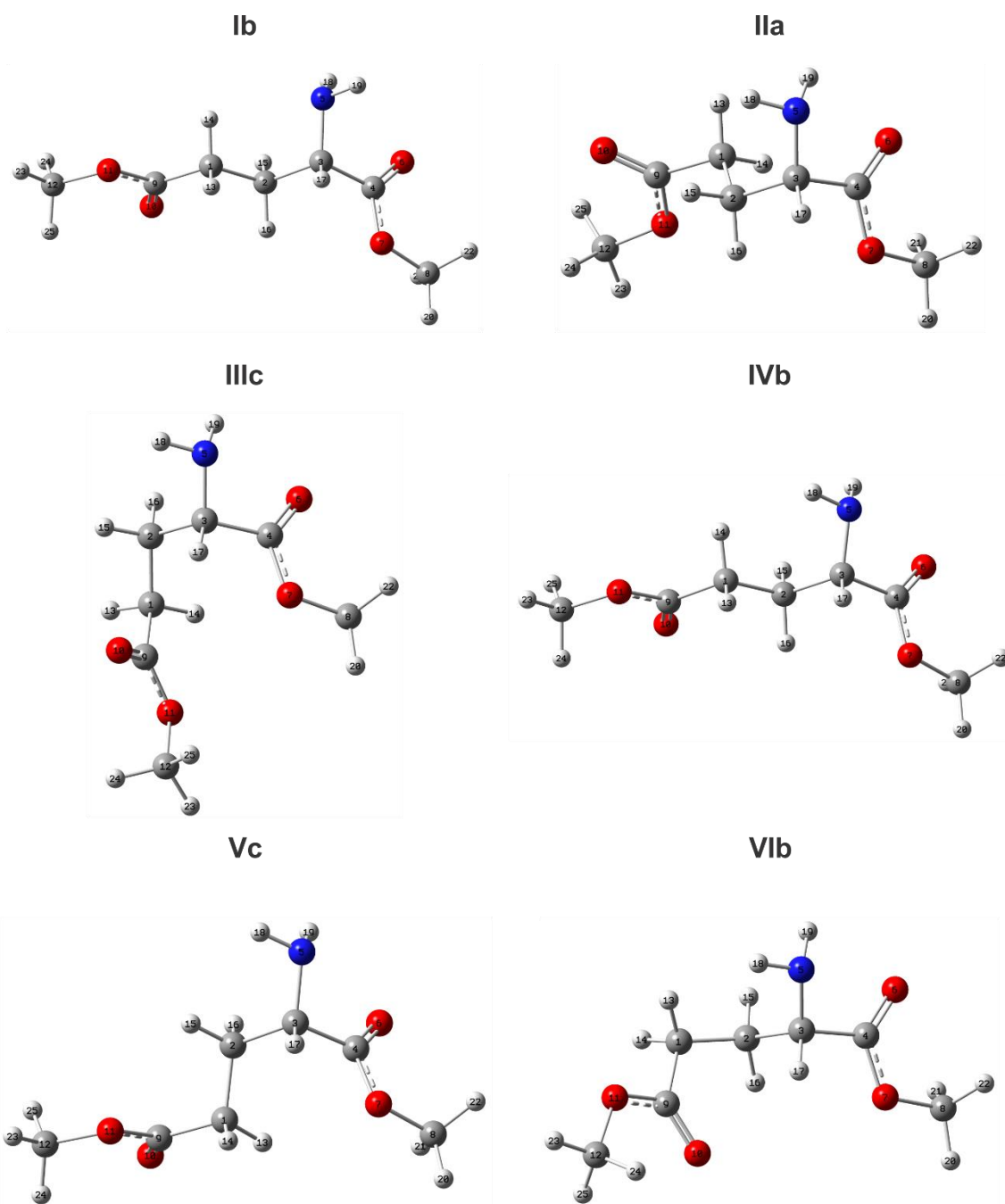


Figure S19 Conformers of GluOMe obtained theoretically at the ω B97X-D/aug-cc-pVTZ level of theory.

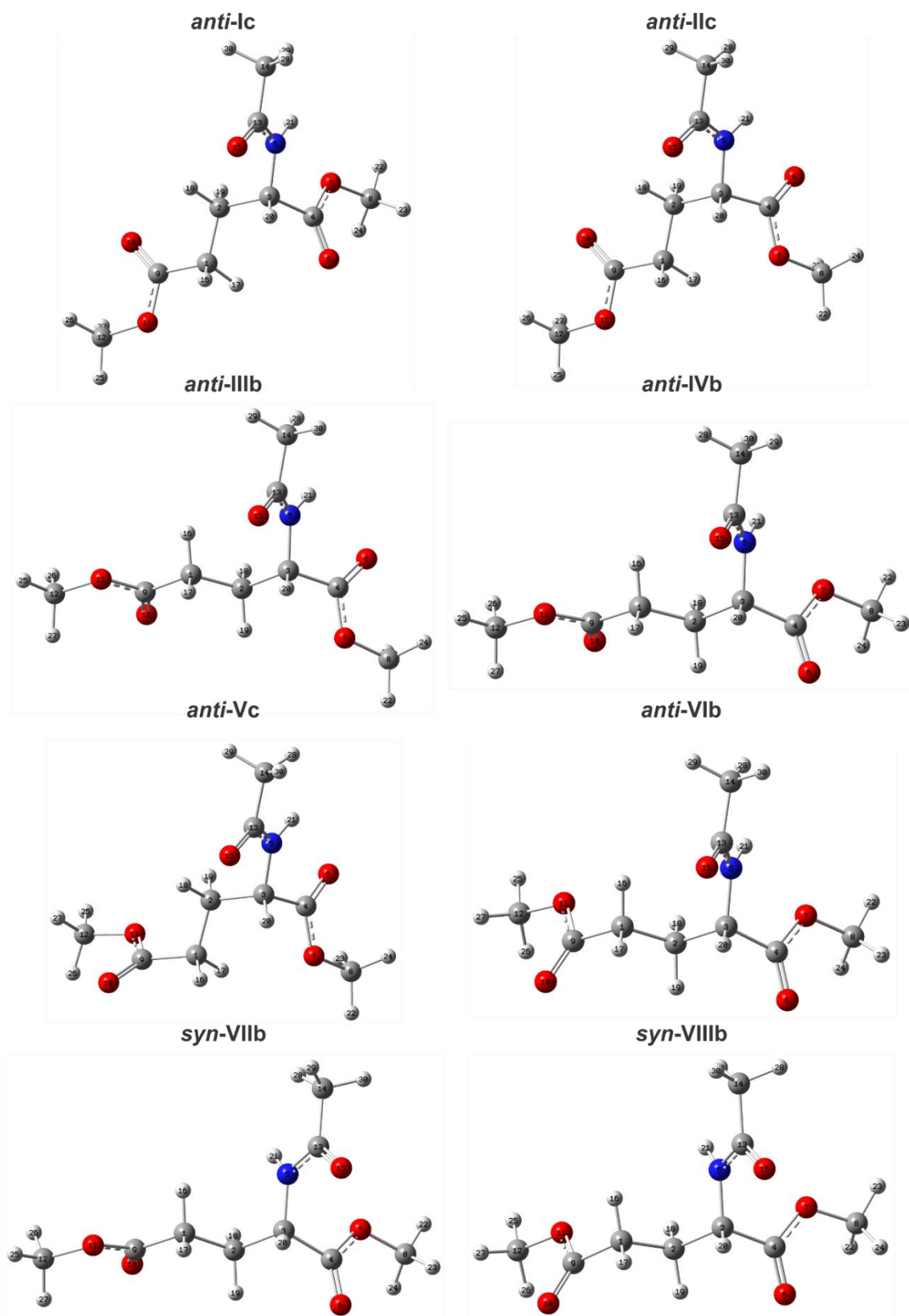


Figure S20 Conformers of AcGluOMe obtained theoretically at the ω B97X-D/aug-cc-pVTZ level of theory.

Table S1 Geometric parameters calculated at the ω B97X-D/aug-cc-pVTZ level of theory for the conformers of GluOMe both in isolated phase and in solution (IEF-PCM). Relative Gibbs free energies are given in kcal mol⁻¹, populations P in % and dihedral angles in degrees.

Conf.	Isolated		CHCl ₃		CH ₂ Cl ₂		CH ₃ CN		DMSO		Dihedral angle	
	Δ G	P	Δ G	P	Δ G	P	Δ G	P	Δ G	P	Ha—C—C—H _{b1}	Ha—C—C—H _{b2}
Ib	0.00	79.1	0.00	72.9	0.00	71.5	0.00	63.2	0.00	62.6	-66.90	176.67
IIa	—	—	1.36	7.3	1.59	5.0	1.64	4.0	1.65	3.9	63.46	-52.60
IIIc	1.22	10.1	1.38	7.0	1.45	6.2	1.36	6.3	1.35	6.4	174.82	59.31
IVb	1.98	2.8	1.52	5.6	1.34	7.4	0.97	12.3	0.94	12.8	-64.09	179.30
Vc	2.34	1.5	1.75	3.8	1.46	6.1	1.37	6.2	1.42	5.7	-179.20	64.88
VIb	1.48	6.5	1.81	3.4	1.73	3.8	1.22	8.0	1.17	8.6	-64.37	178.58

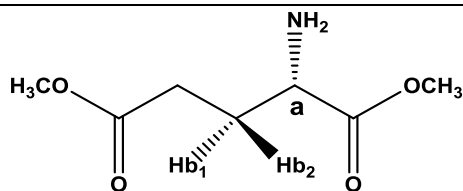
Table S2 Geometric parameters calculated at the ω B97X-D/aug-cc-pVTZ level of theory for the conformers of AcGluOMe both in isolated phase and in solution (IEF-PCM). Relative Gibbs free energies are given in kcal mol⁻¹, populations P in % and dihedral angles in degrees.

Conf.	Isolated		CHCl ₃		CH ₂ Cl ₂		CH ₃ CN		DMSO		Dihedral angle	
	ΔG	P	ΔG	P	ΔG	P	ΔG	P	ΔG	P	Ha—C—C—H _{b1}	Ha—C—C—H _{b2}
<i>anti-Ic</i>	1.3	5.4	0.0	28.6	0.9	5.9	1.0	6.0	1.3	4.4	-174.15	70.34
<i>anti-IIc</i>	0.0	47.5	0.0	27.4	0.0	29.2	0.0	32.6	0.3	27.1	-174.30	70.58
<i>anti-IIIb</i>	0.2	36.3	0.5	11.8	0.9	6.6	0.9	7.0	1.0	8.2	-62.94	-179.52
<i>anti-IVb</i>	1.5	3.8	0.5	11.4	0.0	28.9	0.0	30.5	0.0	41.8	-67.85	175.62
<i>anti-Vc</i>	1.2	6.1	0.7	8.2	1.0	4.9	1.1	5.0	1.4	4.2	-175.25	69.11
<i>anti-VIb</i>	2.3	0.9	0.9	6.6	0.7	9.0	1.3	3.7	1.3	4.8	-66.17	176.62
<i>syn-VIIb</i>	—	—	1.2	4.0	0.5	12.8	1.0	6.4	1.0	7.7	69.10	174.67
<i>syn-VIIIb</i>	—	—	1.5	2.1	1.4	2.7	0.8	8.9	1.8	1.9	-67.77	175.58

Table S3 Calculated populations (ω B97X D/aug-cc-pVTZ) of conformers **a**, **b** and **c** in the conformational equilibrium of GluOMe in both isolated phase and in different solvents (CHCl₃, CH₂Cl₂, CH₃CN and DMSO).

Conformers	Isolated	CHCl ₃	CH ₂ Cl ₂	CH ₃ CN	DMSO
a	0.0	7.3	5.0	4.0	3.9
b	88.4	81.9	82.7	83.5	84.0
c	11.6	10.8	12.3	12.5	12.1

Table S4 Experimental and theoretical ^1H NMR data obtained for GluOMe in the different studied solvents. Chemical shifts (δ) and $^3J_{\text{HH}}$ coupling constants are given in ppm and Hz, respectively. ϵ is the solvent dielectric constant.



Solvent	ϵ	δH_a	$^3J_{\text{HaHb1,calc}}$	$^3J_{\text{HaHb2,calc}}$	Average	$^3J_{\text{HaHb1,obs}}^a$	$^3J_{\text{HaHb2,obs}}^a$
CDCl_3	4.8	3.99	3.3	10.3	6.8	6.2	6.2
CD_2Cl_2	9.1	3.96	3.3	10.2	6.7	6.3	6.3
CD_3CN	37.5	3.82	3.2	10.1	6.6	6.4	6.4
$\text{DMSO-}d_6$	46.7	3.74	3.2	10.2	—	6.4	7.0

^aError in measurements of $J = \pm 0.1$ Hz.

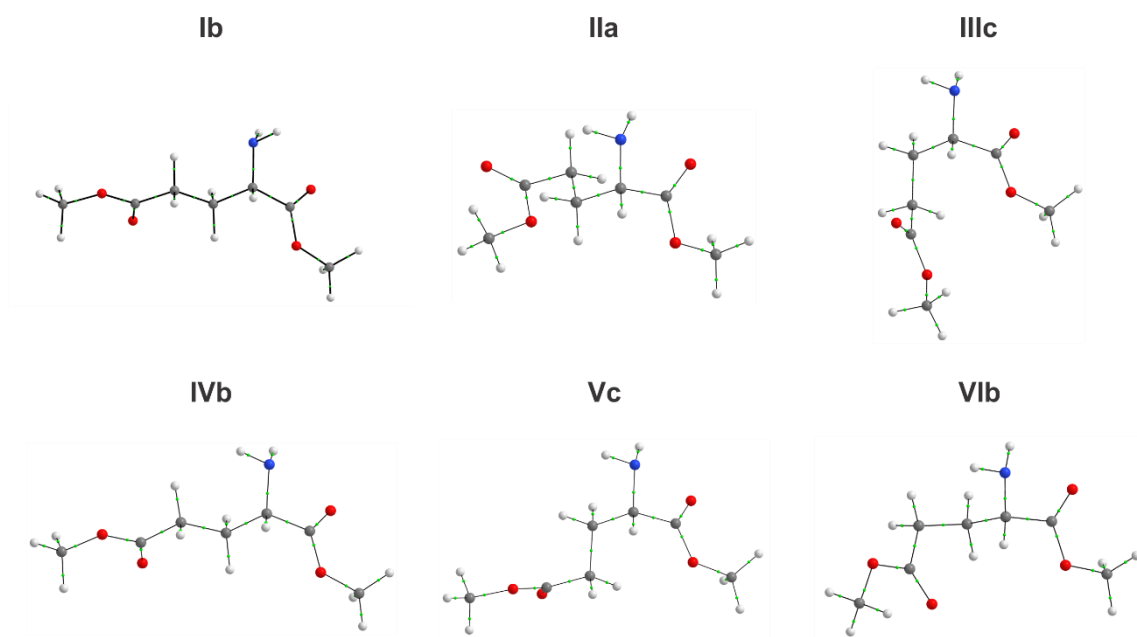


Figure S21 QTAIM molecular graphs for the conformers of GluOMe.

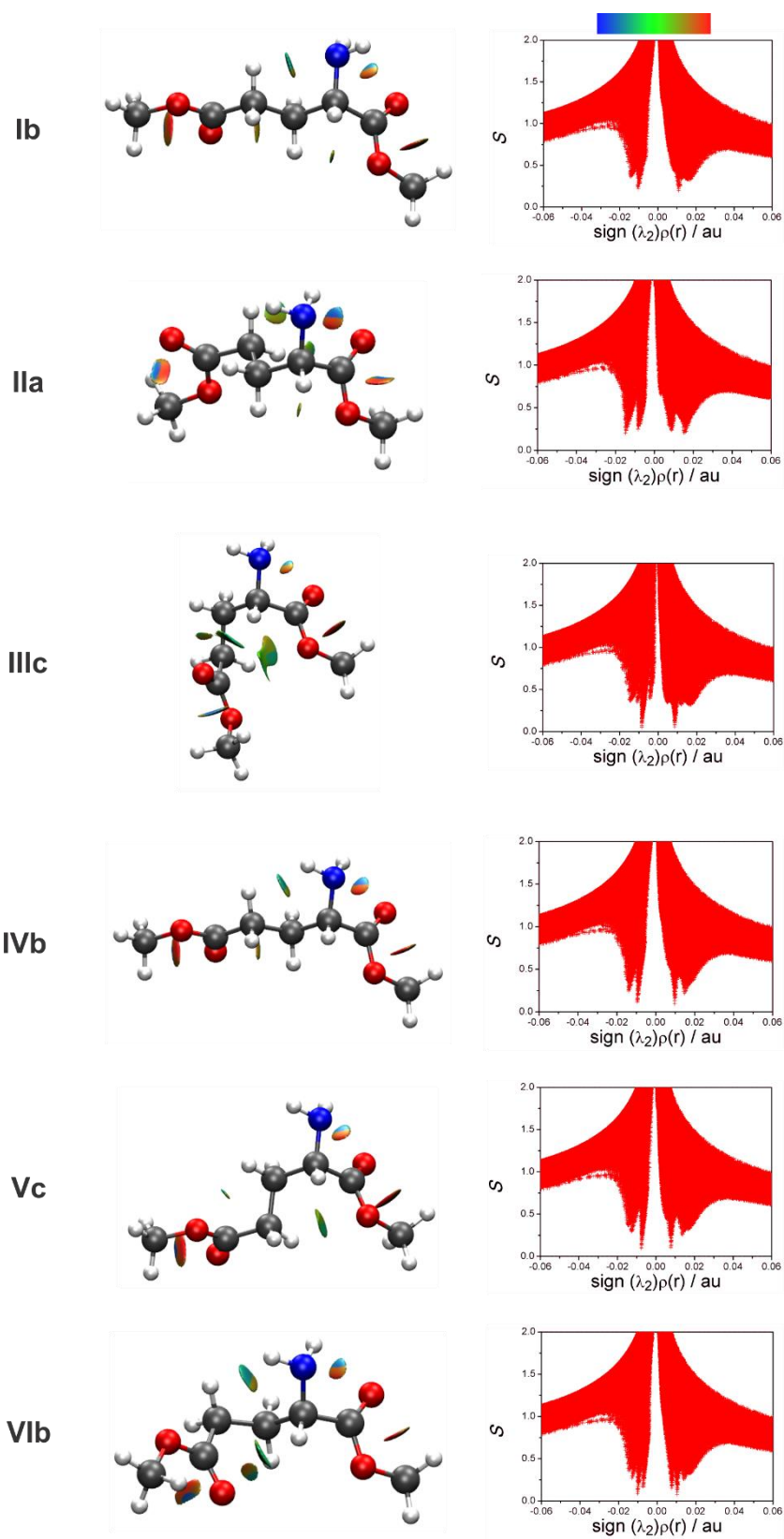


Figure S22 NCI isosurfaces generated with $S = 0.5$ au and blue-green-red scaling from $-0.02 < (\lambda_2)\rho(r) < 0.02$ au, and NCI plots of the reduced density gradient S versus $\text{sign}(\lambda_2)\rho(r)$ for the conformers of GluOMe.

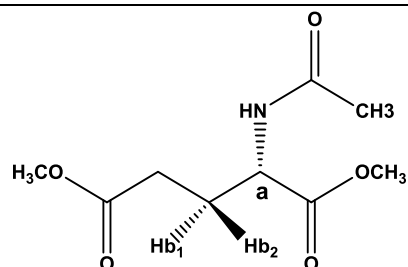
Table S5 NBO parameters obtained at the ω B97X-D/aug-cc-pVTZ level for the conformers of GluOMe. Lewis, hyperconjugative and second order perturbation $LP_2(O) \rightarrow \sigma^*_{NH}$ energies are given in kcal mol⁻¹. The energy threshold for the interactions is equal to 0.05 kcal mol⁻¹.

Conformer	Isolated		CHCl ₃		DMSO		$LP_2(O) \rightarrow \sigma^*_{N5H18^a}$	$LP_2(O) \rightarrow \sigma^*_{N5H19^a}$
	E_{Lewis}	E_{Hyper}	E_{Lewis}	E_{Hyper}	E_{Lewis}	E_{Hyper}		
Ib	0.00	2.52	0.74	2.87	0.82	2.60	0.14	—
IIa	5.54	7.07	6.42	7.75	6.54	7.71	0.11	0.21
IIIc	6.92	7.56	5.81	6.51	4.28	5.13	0.19	0.30
IVb	—	—	4.06	4.52	3.52	3.87	0.27	0.36
Vc	0.15	0.00	0.00	0.00	0.00	0.00	0.11	0.35
VIb	4.33	4.73	2.60	3.17	1.59	2.28	0.20	0.39

Table S6 Calculated populations (ω B97X-D/aug-cc-pVTZ) of conformers **b** and **c** in the conformational equilibrium of AcGluOMe in both isolated phase and in different aprotic solvents (CHCl₃, CH₂Cl₂, CH₃CN and DMSO).

Conformers	Isolated	CHCl₃	CH₂Cl₂	CH₃CN	DMSO
b	41.0	35.9	60.0	56.5	64.4
c	59.0	64.1	40.0	43.5	35.6

Table S7 Experimental and theoretical ^1H NMR data obtained for AcGluOMe in the different studied solvents. Chemical shifts (δ) and $^3J_{\text{HH}}$ coupling constants are given in ppm and Hz, respectively. ϵ is the solvent dielectric constant.



Solvent	ϵ	δH_a	$^3J_{\text{HaHb1,obs}}^a$	$^3J_{\text{HaHb1,calc}}$	$^3J_{\text{HaHb2,obs}}^a$	$^3J_{\text{HaHb2,calc}}$
CDCl_3	4.8	4.63	7.9	8.2	5.2	6.7
CD_2Cl_2	9.1	4.55	5.3	5.9	8.0	8.8
CD_3CN	37.5	4.37	5.3	6.3	8.7	8.5
$\text{DMSO-}d_6$	46.7	4.24	5.4	5.6	8.9	9.1
D_2O	78.5	4.36	5.3	—	9.1	—

^aError in measurements of $J = \pm 0.2$ Hz.

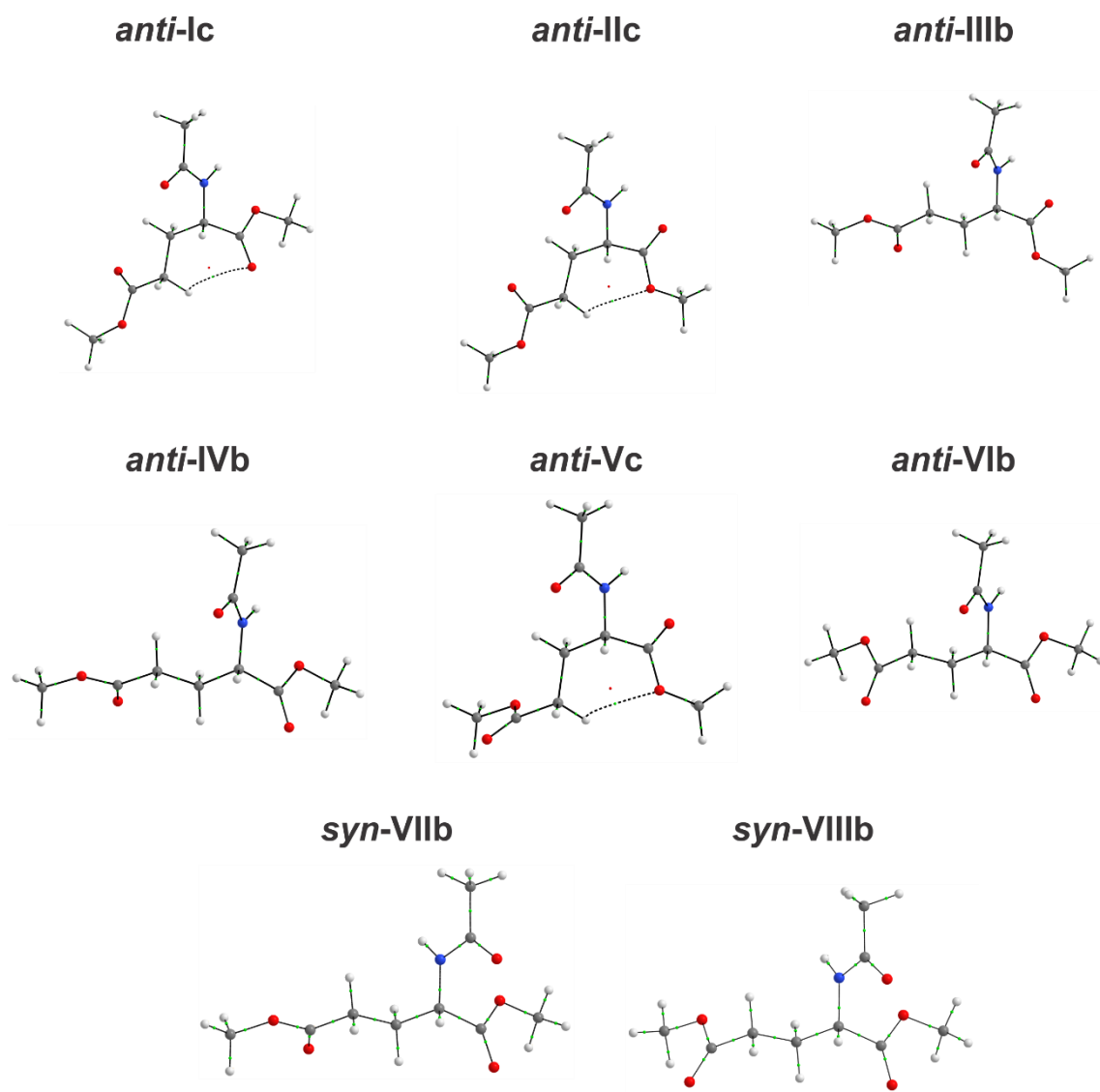
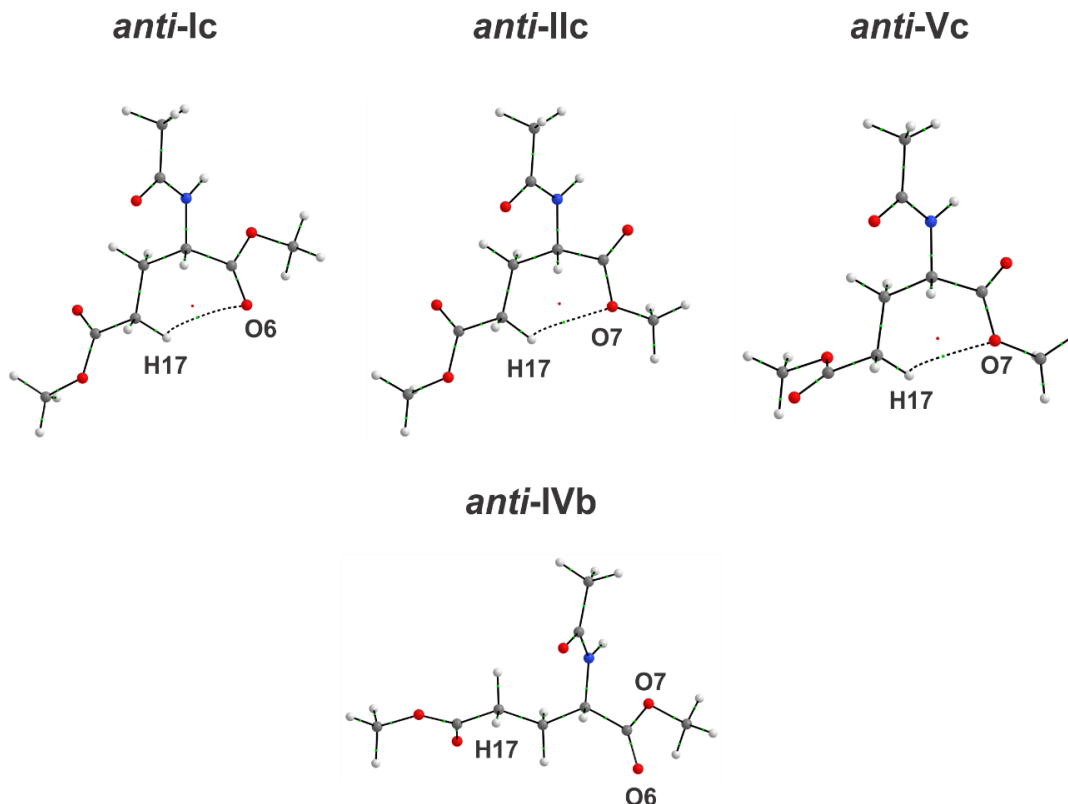


Figure S23 QTAIM molecular graphs for the conformers of AcGluOMe.

Table S8 QTAIM parameters (in au) for the conformers *anti-Ic*, *anti-IIc*, *anti-Vc* and *anti-IVb* (reference).

Parameter	<i>anti-Ic</i>		<i>anti-IIc</i>		<i>anti-Vc</i>		<i>anti-IVb</i>
$\rho(\mathbf{r})$	+0.0098		+0.0106		+0.0102		—
$\nabla^2\rho(\mathbf{r})$	+0.0367		+0.0399		+0.0382		—
ε	+0.7271		+0.2233		+0.2695		—
	H17	O6	H17	O7	H17	O7	H17
$q(\mathbf{H})$	+0.0499	—	+0.0389	—	+0.0278	—	+0.0412
$M_I(\mathbf{H})$	+0.1232	—	+0.1237	—	+0.1269	—	+0.1306
$E(\mathbf{H})$	-0.6058	—	-0.6125	—	-0.6170	—	-0.6093
$V(\mathbf{H})$	+43.01	—	+43.21	—	+44.09	—	+45.85
r^0	2.53	3.28	2.53	3.37	2.53	3.37	—
r	2.04	2.79	1.97	2.70	2.05	2.73	—
Δr	0.46	0.50	0.53	0.64	0.45	0.60	—

$\rho(\mathbf{r})$ = electron density; $\nabla^2\rho(\mathbf{r})$ = laplacian of the electron density; ε = ellipticity; $q(\mathbf{H})$ = atomic electric charge; $M_I(\mathbf{H})$ = atomic first dipole moment; $E(\mathbf{H})$ = atomic energy; $V(\mathbf{H})$ = atomic volume; r^0 = van der Waals radius of the atom when involved in a hydrogen bond; r = van der Waals radius of the atom when not involved in a hydrogen bond; $\Delta r = r^0 - r$.



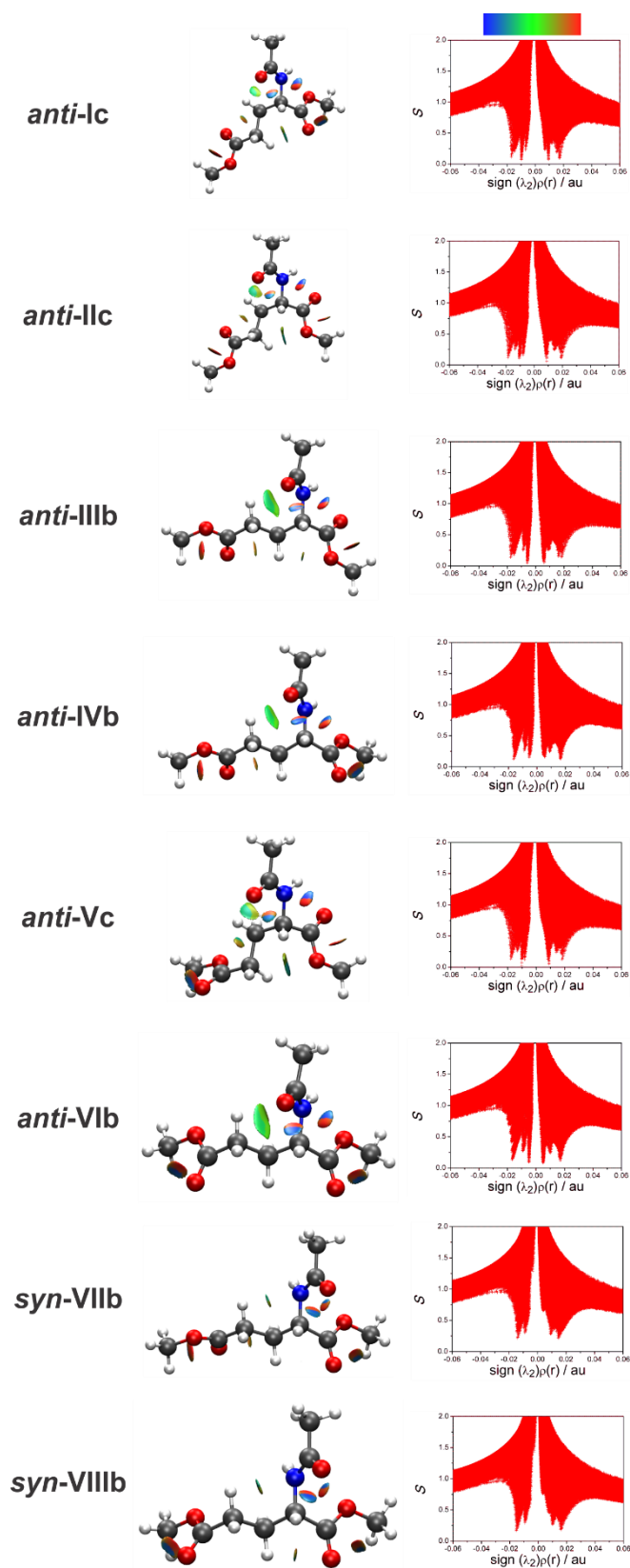


Figure S24 NCI isosurfaces generated with $S = 0.5$ au and blue-green-red scaling from $-0.02 < (\lambda_2)\rho(r) < 0.02$ au, and NCI plots of the reduced density gradient S versus $\text{sign}(\lambda_2)\rho(r)$ for the conformers of AcGluOMe.

Table S9 Hyperconjugative interactions, in kcal mol⁻¹, for the conformers of AcGluOMe obtained through the NBO calculations at the ω B97X-D/aug-cc-pVTZ level of theory. The energy threshold for the interactions is equal to 0.05 kcal mol⁻¹.

Conf.	LP ₁ (O6) → σ^* _{N5H21}	LP ₂ (O6) → σ^* _{N5H21}	LP ₁ (O7) → σ^* _{N5H21}	LP ₂ (O7) → σ^* _{N5H21}	LP ₁ (O) → σ^* _{C1H17}	LP ₂ (O) → σ^* _{C1H17}
<i>anti-Ic</i>	—	—	0.59	—	0.08	0.09
<i>anti-IIc</i>	0.29	1.00	—	—	0.26	0.14
<i>anti-IIIb</i>	0.21	0.81	—	—	—	—
<i>anti-IVb</i>	—	—	0.39	—	—	—
<i>anti-Vc</i>	0.25	0.88	—	—	0.05	0.16
<i>anti-VIb</i>	—	—	0.42	—	—	—
<i>syn-VIIb</i>	—	—	—	—	—	—
<i>syn-VIIIb</i>	—	—	—	—	—	—

Table S10 NBO parameters obtained at the ω B97X-D/aug-cc-pVTZ level for the conformers of AcGluOMe. Lewis and hyperconjugative energies are given in kcal mol⁻¹.

Conf.	Isolated		CHCl ₃		DMSO	
	E _{rel,Lewis}	E _{rel,Hyper}	E _{rel,Lewis}	E _{rel,Hyper}	E _{rel,Lewis}	E _{rel,Hyper}
<i>anti-Ic</i>	0.69	1.38	0.64	0.91	0.00	0.00
<i>anti-IIc</i>	5.02	7.22	4.42	5.87	3.30	4.28
<i>anti-IIIb</i>	6.43	9.93	5.53	8.00	3.40	5.26
<i>anti-IVb</i>	3.36	4.49	2.81	3.67	2.63	3.40
<i>anti-Vc</i>	2.72	3.84	2.50	3.06	1.86	1.99
<i>anti-VIb</i>	0.00	0.00	0.00	0.00	1.30	1.32
<i>syn-VIIb</i>	—	—	2.75	3.66	3.64	4.76
<i>syn-VIIIb</i>	—	—	0.39	0.40	0.02	0.24